Desalination and Water Treatment
www.deswater.com

doi: 10.5004/dwt.2021.26551

210 (2021) 258–272
January

Use of *Olea europaea* leaves-based activated carbon for pollutant removal from liquid effluents

Oukacha Douinat, Benaouda Bestani*, Nouredine Benderdouche, Ahmed Boucherdoud

Laboratoire de Structure, Elaboration et Application des Matériaux Moléculaires (SEAMM) Faculté des Sciences et de la Technologie, Université Abdelhamid Ibn Badis, Mostaganem, Algeria, Tel. +213 5 52 32 94 07; Fax: +213 45206476; email: bestanib@yahoo.fr (B. Bestani), Tel. +213 7 92 69 65 00; Fax: +213 45206476; email: douinat.oukacha@yahoo.fr (O. Douinat), Tel. +213 7 72 61 89 06; Fax: +213 45206476; email: benderdouchen@yahoo.fr (N. Benderdouche), Tel. +213 7 74 79 51 29; email: bo-ahmed@live.fr (A. Boucherdoud)

Received 4 April 2020; Accepted 1 September 2020

ABSTRACT

Efficient adsorbents preparation from *Olea europaea* leaves by simple surface modification for Rosaniline Base and Chrysoidine R removal from simulated water have been investigated. Separate impregnation of powdered leaves in H_2SO_4 and KOH solutions (30%) followed by pyrolysis (500°C) during 2 h resulted in AH30 and AK30 adsorbents. Operating parameters effecting dyes adsorption such as contact time, adsorbent dose, pH and temperature were studied. Equilibrium data were analyzed using adsorption isotherms. Treatments were found to enhance the adsorption capacity significantly relative to their inactivated state (INACT). Langmuir model is more representative with adsorptive capacities enhancements due to treatments of up to 158.73 and 357.14 mg g^{-1} for CRD and RBD dyes, respectively, by AH30 compared with 129.87 and 270.27 mg g^{-1} by the commercial Merck activated carbon used as a reference. Chemical and physico-chemical methods such as Fourier-transform infrared spectroscopy analyses, ATG/ATD, MEB/EDS, Boehm, iodine number, methylene blue index and pH_{zpc} were performed to characterize the prepared adsorbents prior to their utilization. Adsorption mechanism was found to obey pseudo-second-order kinetic model and the sorption process is controlled by intra-particle diffusion. Thermodynamic analysis of both dyes confirms their spontaneity and exothermicity. These results showed that activated *Olea europaea* leaves prove to be very useful and efficient adsorbent in removing related toxic pollutants from textile wastewater.

Keywords: Surface modification; Adsorption; Agro-waste; Wastewater; Azo dyes

1. Introduction

Even representing a small percentage (about 3%) of water covering the earth, freshwater makes the development of water pollution worldwide so problematic.

It was estimated by the World Water Assessment Programme (UNESCO-WWAP) that about 2 million ton d^{-1} of sewage, industrial and agricultural waste are discharged into the world's water. This waste discharge as pollutants leaves not only a very small portion of accessible fresh water but also causes the death of many organisms and can disrupt entire ecosystems. Pollution caused by organic pollutants becomes a serious problem of environmental degradation, which requires special attention by straightening imposed environmental regulations and guidance provided by the World Health Organization (WHO) and the European Union [1]. Extensively used in different industries, dyes are organic pollutants wide in variety and toxicity that have been of great threat to aquatic organisms, plants and humans once discharged in the environment in the form of

* Corresponding author.

1944-3994/1944-3986 © 2021 Desalination Publications. All rights reserved.

colored wastewater without any prior treatment [2]. Many treatment alternatives for dyes-laden wastewater have been used including physical, chemical, biological and physico-chemical [3–6] such as advanced oxidation, coagulation/flocculation, reverse osmosis, nanofiltration, ion exchange, among others [7–10]. Although well developed, these methods are proved to be less efficient, more costly and generate huge quantity of sludge. As a process, adsorption using activated carbon is one of the most widely used technique that has gained much scientific attention in the last decades due to its high efficiency for organic pollutants removal from wastewater, simplicity to realize, less expensive and easy to scale-up [11–13].

With a highly developed porosity and an extended interparticulate surface area, activated carbons are the most commonly used adsorbents for range of pollutants removal including dyes from wastewater [14–16]. They can be manufactured from a wide variety of raw materials and Agricultural by-products with high percentage of carbon content as a predominant qualification [17–22].

By being lignocellulosic materials with relatively high carbon content, *Olea europaea* leaves, a raw material abundantly available locally, presenting no value and often presenting expensive disposal problems was chosen in this study as an alternative for activated carbon production. The organic pollutants selected to be removed from simulated water were Chrysoidine R, which belongs to the azo dyes category is widely used to dye silk, cotton, varnish, printing inks, chromed leather, and cellulose-ester plastics [23–25]. Also used as a biological stain and as a dye in oils, fats, and waxes for polishes. It is sometimes used illegally as a food additive despite its potential toxicity causing nausea, vomiting and muscle weakness [26,27], and Rosaniline Base, which belongs to the category of magenta dyes, an organic base, used to make the dye fuchsine, extensively used as textile dyes and for sulfur dioxide measurements in the atmosphere. It is toxic and is an irritant that causes dermatitis and conjunctivitis with prolonged skin contact and eye exposure, respectively. Ingestion may cause nausea, gastrointestinal irritation, vomiting and diarrhea [28,29].

Both dyes are toxic and are difficult to biodegrade because of their complex aromatic structures. Prior treatment of wastewater laden with these dyes is necessary before it is discharged into the environment using efficient low-cost material was the aim of this study.

2. Materials and methods

2.1. Materials

Dyes used in this study were Rosaniline base (dye content 70%) and Chrysoidine R (>98%) supplied by REACTIFS RAL. Table 1 shows chemical structures and characteristics of these dyes. Stock solutions (10^{-2} M) were prepared according to standard procedure by dissolving the required amount of each dye separately in distilled water. Working solutions of the desired concentrations were obtained by successive dilutions. Sulfuric acid and potassium hydroxide (purchased from Sigma-Aldrich, Germany) of high purity were used as chemical activators for the preparation of activated carbon.

2.2. Adsorbent preparation

Olea europaea leaves were collected from nearby farms during the olive harvest (autumn), washed thoroughly with tap water to remove dust then with distilled water and dried at 70°C overnight, crushed and sieved to obtain powdered particles with a diameter less than 0.14 mm. In order to enhance their adsorptive properties, *Olea europaea* leaves were chemically treated separately by sulfuric acid (30%) and potassium hydroxide (30%). The mixtures were agitated for 24 h at ambient, filtered, dried and then pyrolyzed at 500°C in tubular furnace (Nabertherm MORETHAN HEAT 30-3000°C) for 2 h (heating speed: 10°C/min). The obtained samples were washed with hot distilled water, dried overnight and kept in desiccators before adsorption tests.

2.3. Adsorbents characterization

2.3.1. Surface area estimation

Usually used for their experimental simplicities as a relative indicator of adsorbents available surface area, iodine and methylene blue adsorption onto activated carbons can be very useful for adsorbent structure. First, the iodine number is quick test giving an indication of the internal surface area of virgin activated carbon so it is mainly adsorbed in the micropores since the surface area occupied by one molecule is equal to 20.96 $Å^2$ [30]. It is widely used as a quality control parameter in production and reactivation of activated carbons. It is defined as the quantity in mg of iodine adsorbed by 1 g of material when the iodine residual concentration of the filtrate is 0.02 ± 0.01 N according to ASTM D 4607 standard method [31], which is based on a three-point isotherm. A standard iodine solution (0.1 ± 0.01 N) was treated with three different weights of adsorbent. The sample was treated with 10 mL of 5% (V/V) HCl. The mixture was boiled for 30 s, and then cooled at room temperature. 100 mL of 0.1 N iodine solution was immediately added to the mixture and stirred for 30 s. The solution was then filtered and 50 mL of the filtrate was titrated with 0.1 N (0.05 mol L^{-1}) sodium thiosulfate solution using thyodene (or starch) as an indicator. The amount of iodine adsorbed per gram of adsorbent is plotted against the residual iodine concentration, using logarithmic axes. If the residual iodine concentration was not within the range (0.008–0.04 N), the procedure is repeated using different carbon masses for each isotherm point. A regression analysis was applied to the three points and the iodine number was calculated as the amount adsorbed at a residual iodine concentration of 0.02 N. Second, methylene blue is a typical dye used to calculate the accessible surface of sorbents to large molecules (mesopores) according to standard method Chemviron Carbon, (Zoning Industriel C. B-7181 Feluy, Belgium) in which one determines the adsorption of the filtrate containing the residual concentration of the methylene blue after contact time of 30 min with the activated carbon. The available surface with methylene blue is calculated by the following equation [32,33]:

$$S_{\mathrm{BM}} = \frac{b \times N_A \times A_{\mathrm{BM}}}{M_{\mathrm{BM}}} \quad (1)$$

where S_{BM} is the surface area ($m^2\ g^{-1}$), b is maximum adsorption capacity (mg g^{-1}) based on a monolayer coverage (determined previously from the Langmuir model), N_A is Avogadro's number ($6.023 \times 10^{23}\ mol^{-1}$), A_{BM} is the surface occupied by a molecule of methylene blue (taken as 119 $Å^2 = 1.19 \times 10^{-18}\ m^2$), and M_{BM} is the molecular weight of methylene blue (319.86 g mol^{-1}).

2.3.2. pH_{zpc} and Boehm titration

The zero point charge of the carbon (pH_{zpc}) defined as being the pH for which there is absence of positive or negative charge on the activated carbon surface was determined as follows: volumes of 50 mL of 10^{-2} M NaCl aqueous solution were placed in a series of stoppered conical flasks. The initial pH value (pH_i) of each solution was then adjusted between 2 and 12 by using dilute sodium hydroxide or hydrochloric acid solutions and accurately noted. An amount of 0.15 g activated carbon was then added to each flask, stirred for 48 h and then the final pH (pH_f) was measured for each solution. The difference between the initial and final pH value ($\Delta pH = pH_i - pH_f$) was plotted against (pH_i).

2.3.3. Surface functional groups determination

In order to identify the principle functional groups present at the surface of adsorbents, the infra-red analysis was used. The IR spectra were determined using sampling in KBr on an IRPrestige-21, Shimadzu UVmini-1240 UV–vis spectrophotometer (Shimadzu Co., Ltd., Tokyo, Japan). Second, Boehm method was used for acidic sites quantification (back-titration of HCl by NaOH) and for basic sites quantification (direct titration of HCl by NaOH) [34]. In addition, scanning electronic microscopy observations: scanning electron microscopy (SEM) analysis was performed on HIROX SH-400 M SEM-EDS BRUKER XFlash® 6 | 60 Detector Nano-analysis N°. 8535 (Germany) spectrometer for sample characterization.

3. Adsorption experiments

For highest adsorption capacities of Rosaniline base and Chrysoidine R onto considered activated carbons, the influence of important parameters including adsorbent dosage (2–16 mg L^{-1} range), contact time (30–360 min range), pH (2–12 range) and temperature (298.15, 303.15 and 313.15 K) were investigated. These experiments were performed by batch sorption in a series of capped 250 mL Erlenmeyer flasks. For such sorption studies, a 25 mL volume of a dye solution of known initial concentration prepared from stock solution (10^{-2}M) by dilution was mixed with a known amount of adsorbent; the mixture was agitated magnetically at a constant speed of 400 rpm until equilibrium had been reached, then centrifuged at 4,000 rpm and the supernatant concentration determined using a Optizen 2120 UV spectrophotemeter, (Korea) at λ_{max} values mentioned in Table 1. Solutions were diluted as required so that their absorbance remained within the linear calibration range (Beer–Lambert law). Experiments were repeated in triplicate and the average values were reported. Dye uptakes (q_e) in mg g^{-1} were determined according to the following mass balance relationship:

$$q_e = \frac{(C_0 - C_{eq})\ V}{1{,}000\ m} \tag{2}$$

where C_0 and C_{eq} are the initial and the equilibrium dye concentration (mg L^{-1}), V is the volume of the liquid phase (mL) and m is the mass of the activated carbon sample (g).

4. Results and discussion

4.1. Samples characterization

All samples were characterized prior to adsorption tests using different chemical and physico-chemical methods such

Table 1
Chemical structure and characteristics of adsorbed dyes

	Chrysoidine R	Rosaniline Base
Structure	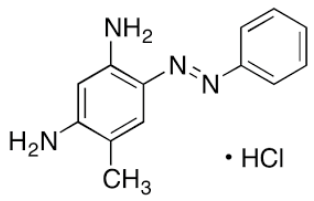	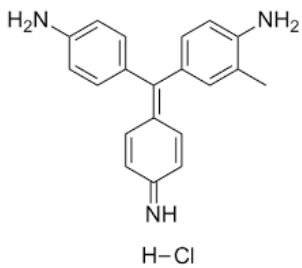
Molecular formula	$C_{13}H_{15}ClN_4$	$C_{20}H_{19}N_3HCl$
Molecular weight (g mol^{-1})	262.73	337. 86
Color index (C.I.)	11,320	42,510
Maximum wavelength λ_{max} (nm)	450	542
Classification	Azo dye	Magenta dye
CAS number	4438-16-8	632-99-5

as Fourier-transform infrared spectroscopy (FT-IR) analyses, ATG/ATD, MEB/EDS, Boehm, iodine number, methylene blue index and pH_{zpc}.

4.1.1. Functional groups identification by FT-IR spectroscopy

FT-IR analysis spectra of the all samples shown in Fig. 1 were obtained by IR Prestige-21 Shimadzu Corporation, (Japan) to determine the prepared AH30 and AK30 samples functional groups. A mixture of KBr (100 mg) and powdered samples (1 mg) was compressed for spectra analysis in the 4,000–400 cm^{-1} range. Before activation, the spectrum of INACT biosorbent showed high intensity peaks around 3,609 and 3,311 cm^{-1} corresponding to the stretching vibration of hydroxyl groups and the primary aliphatic amine, respectively. Medium intensity peaks around 2,921; 1,635 and 1,600 cm^{-1} characteristic of C–H stretching (alkane), C–H stretching (aldehyde) and C–C stretching (alkane), respectively. Weak peaks are present around 2,848 cm^{-1} of aliphatic (C–H) elongation. Other weak peaks at 1,379; 1,309; 1,105 and 1,004 cm^{-1} attributed to the elongation of (C–O) in the acid groups, alcohols, phenols, ethers and esters.

After activation with the sulfuric acid and hydroxide potassium followed the heat treatment, peaks between 3,600 and 3,300 cm^{-1} disappear creating then new oxygenated groups that can significantly enhance dyes removal. Table 2 summarizes the main functional groups as observed from FT-IR spectroscopy analysis.

4.1.2. pH_{zpc} and Boehm titration

Due to the increase of interest in the solution pH during adsorption processes, a common method used to indicate the net surface charge of the adsorbent in solution is the point of zero charge (pH_{zpc}), pH for which the net surface charge of adsorbent is equal to zero. It is an important parameter for prediction of affinity between adsorbent and adsorbate. The adsorbent surface is considered to be charged positively at $pH < pH_{zpc}$ and negatively charged at $pH > pH_{zpc}$. It is indicated by the intersection point of (pH_{final} vs. $pH_{initial}$ plot) and ($pH_{final} = pH_{initial}$ line) as shown in Fig. 2. It is also related to functional groups (acid or base) on the adsorbent surface usually determined by Boehm titration. As shown in Table 3, the inactivated *Olea europaea* leaves (INACT) have more acid groups (8.08 mmol g^{-1}) than basic ones (6.80 mmol g^{-1}) increasing then the density of negative charge on the surface which favors cationic dyes adsorption such as Rosaniline Base and Chrysoidine R. Acidic (H_2SO_4) and basic (KOH) treatments increase acidic groups and basic groups by 60% and 53%, respectively. This is consistent with high adsorption capacities obtained by AH30.

4.1.3. Mesoporous and microporous available areas

Mesoporous and microporous available areas were determined through a laboratory procedure reported in previous works [30] particularly those with small molecules. Due to its small surface area occupied by one molecule, iodine adsorption (called iodine number) onto the prepared samples is a good indication of their micro-porosity [32] since it has been reported in the literature that 1 mg of iodine adsorbed is almost equal 1 m^2 g^{-1} [35]. Values of iodine number and methylene blue index S_{BM} are summarized in Table 4. The inactivated sample has the lowest iodine number of 320.46 m^2 g^{-1} as expected since most pores are initially filled with impurities. After activations, there

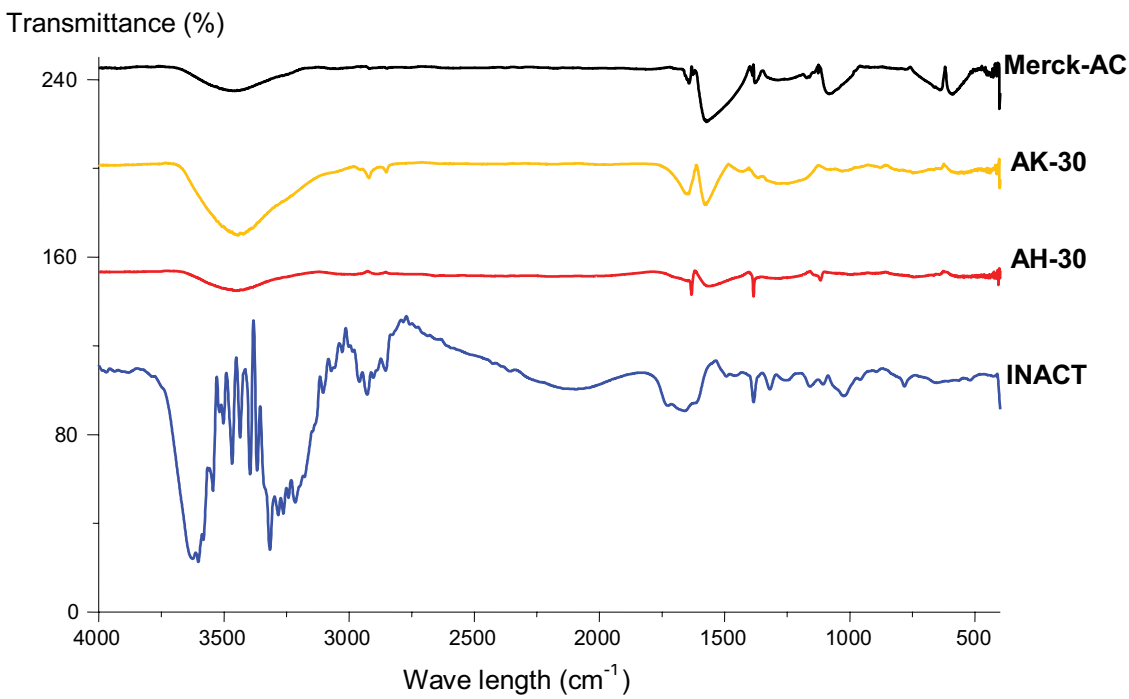

Fig. 1. FT-IR spectrum of all samples.

Table 2
Characteristics of FT-IR wave numbers for INACT, AK30, AH30 and AC-Merck

Adsorbent	Wave number (cm^{-1})	Assignment	Comments
INACT	3,609	O–H stretching, alcohol (strong, sharp)	Free
	3,311	N–H stretching primary aliphamine, medium	
		O–H stretching, alcohol strong, broad	Intermolecular bonded
	2,921	C–H stretching alkane, medium	
	2,848	C–H stretching aldehyde, medium	Doublet
	1,635	C–C stretching alkane, medium	Disubstituted (cis)
	1,600	N–H bending, amine	
	1,379	C–H bending, alkane, medium	Gem dimethyl
	1,309	C–N stretching, arom. amine strong	
	1,105	C=C bending, alkene	Monosubstituted
	1,004	C=C bending, alkene, strong	Monosubstituted
AK30	3,415	O–H stretching, strong band	Intermolecular bonded
	1,639	C=C stretching, medium	Disubstituted (cis)
	1,571	C=C stretching, cyclic alkene, medium	
AH30	1,250	C–N stretching medium	
AC-Merck	3,432	O–H stretching, strong, broad	Intermolecular bonded
	1,558	N–H bending, medium	
	1,063	S=O stretching	

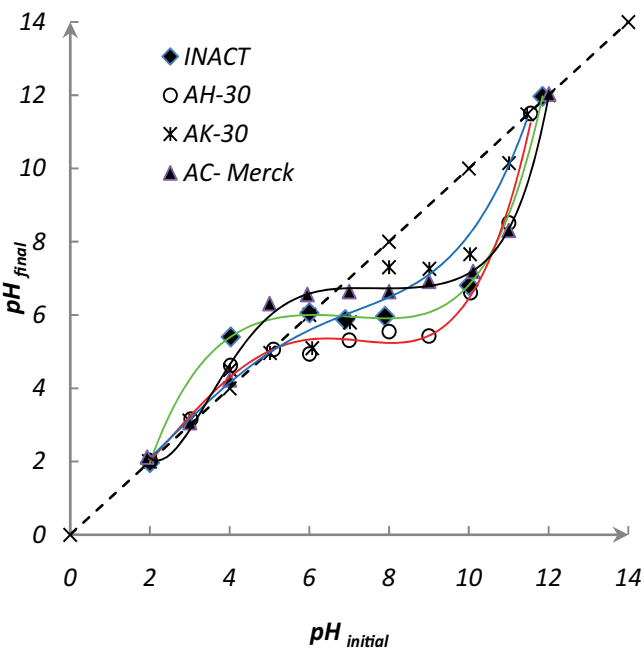

Fig. 2. pH_{zpc} of samples used in this study.

are significant improvement of the iodine number for up to 1,150.07 and 679.04 mg g^{-1} by acid and base treatments, respectively, creating more pores in sample structures. These values are in accordance with the amount of dyes adsorbed. By being a large molecule methylene blue is used to define the macro-porosity available surface of activated carbons [36]. Values of Methylene blue index decreases from the inactivated leaves to the chemically treated ones, this is due may be to the creation of more microporous space.

Table 3
Boehm functional groups and pH_{zpc} of studied samples

	Adsorbents			
Functional groups (mmol g^{-1})	INACT	AH30	AK30	M-AC
Carboxylic	6.93	20.10	20.05	6.73
Lactonic	0.23	0.05	0.15	0.03
Phenolic	0.87	2.05	0.50	0.57
$Total_{Acid\ groups}$	8.03	22.20	20.70	7.33
$Total_{Basic\ groups}$	6.80	21.80	20.20	6.80
pH_{zpc}	6.0	5.1	5.0	6.6

4.1.4. Sample surface morphology

The microstructure of the produced samples was examined by SEM. Fig. 3 shows SEM images of the raw material (INACT sample), the derived activated carbons (AH30 and AK30) and the commercial activated carbon from Merck KGaA, Darmstadt, Germany (AC-Merck), in which there is major difference between the raw and the prepared adsorbents. The surface of the raw material shown in Fig. 3a was fairly smooth, with almost no voids or cavities. However, those of AH30 and AK30 (Figs. 3b and c) activated carbons show that chemical followed by heat treatments produce new external surfaces with pores and cavities leading then to high porosity development (confirmed by iodine number determination: Table 4) as a result of the treatments by chemical reagents (H_2SO_4 and KOH) and evaporation during pyrolysis of some volatile organic components leaving more empty spaces. This increase in porosity is also due to the elimination of some hetero-atoms present initially in the raw material during the heating process as show in

Table 4
Langmuir and Freundlich parameters for both dyes removal and porous available areas of the prepared adsorbents

	Model	Parameters	AH30	AK30	Merck-AC	INACT
Chrysoidine R	Langmuir	R^2	0.99	0.99	0.99	0.99
		b (mg g^{-1})	158.73	113.64	129.87	97.09
		K_L (L mg^{-1})	0.034	0.017	0.069	0.009
		% Enhancement	63.48	17.14	33.76	//
	Freundlich	R^2	0.89	0.98	0.87	0.96
		n	2.31	2.61	5.10	1.93
		K_L (mg g^{-1})	14.23	10.09	40.35	4.15
Rosaniline Base	Langmuir	R^2	0.99	0.99	0.99	0.99
		b (mg g^{-1})	357.14	175.44	270.27	147.06
		K_L (L mg^{-1})	0.233	0.08	0.264	0.073
		% Enhancement	142.85	19.29	83.78	//
	Freundlich	R^2	0.76	0.96	0.84	0.91
		n	3.22	2.67	3.44	2.52
		K_L (mg g^{-1})	96.53	29.37	77.15	21.67
Iodine number (mg g^{-1})			1,150	680	863	321
Methylene Blue index			77	81	186	89
S_{BM} (m^2 g^{-1})			170	184	415	197

the EDS spectra and the chemical composition (Figs. 3a–d). Same phenomena were observed for AC-Merck surface used in this study as a reference.

4.2. Effect of operating conditions on dyes adsorption

4.2.1. Effect of adsorbent dose

Usually used to predict the treatment cost of activated carbon per unit of dye solution, the carbon dose is particularly an important parameter in the sorbent–sorbate equilibrium determination. The dependence of Rosaniline Base and Chrysoidine R dyes uptakes onto the adsorbent dosage was studied by varying the amount of all samples including the inactivated one within the range of 2–16 mg L^{-1} and maintaining all other parameters constant. At early stage of adsorption, efficiency increases, then stabilizes at values representing maximum % removals of 99.92, 99.58 and 94.76 of Rosaniline Base onto AH30, AC-Merck and AK30, respectively, at an adsorbent dosage of 4 g L^{-1} (figures not shown). However, removal efficiencies of 99.92%, 99.24% and 97.77% of Chrysoidine R were achieved using AH30, AC-Merck and AK30, respectively, at 6 g L^{-1} adsorbents dosage. While, lowest removal values of both dyes were obtained at 6 g L^{-1} by INACT sample as expected. In general, uptake increases with increasing adsorbent dosage. This increase in adsorption rate can be attributed to the availability of a greater number of adsorption sites due to activation leaves compared with the inactivated ones. By increasing adsorbent dose, particles aggregate resulting in lower uptakes.

4.2.2. Effect of solution pH

Another critical parameter affecting the adsorption process is the external solution pH. Varying the later can easily modify the adsorbent surface charge as reported in the literature [47]. In order to determine the optimum pH conditions for both the dyes onto the prepared adsorbents, initial pH of the solution of known volume and concentration was placed in a beaker and was varied from 2 to 12 by adding either dilute NaOH or HCl (0.1 N) solutions. Then a certain volume of this solution was placed in a flask to which a certain amount of adsorbent (dose determined previously) was added and the mixture was shaken then filtered and the dyes concentration was determined by spectrophotometry. As shown in Fig. 4, there was no major effect on the uptake of Chrysoidine R and Rosaniline Base by the AH30, where both dyes were almost entirely adsorbed (99.95%) at initial pH. For the remaining adsorbents, dye uptakes increased with increasing pH values until saturation. At low pH, lower adsorption capacities were attained due to the strong acid environment (competition between high concentrations of H^+ competing with cationic dye molecules). While a significant increase in adsorption capacity was observed as pH increases. This is due may be to high concentration to the weak acid environment competing with the dye molecules (cationic) for the available sites which favor an attraction between both adsorbent surface and the positively charged dye [22].

4.2.3. Effect of contact time

It was found that the percentage removal of both dyes by all adsorbents increases with increasing time until equilibrium is reached corresponding to 100 min for Chrysoidine R and 90 min for Rosaniline Base. Fig. 5 shows the case of Chrysoidine R adsorption by all the considered adsorbents where the saturation occurs at the above-mentioned time except for the case of AH30 where there is almost no time effect. As a consequence, subsequent adsorption experiments

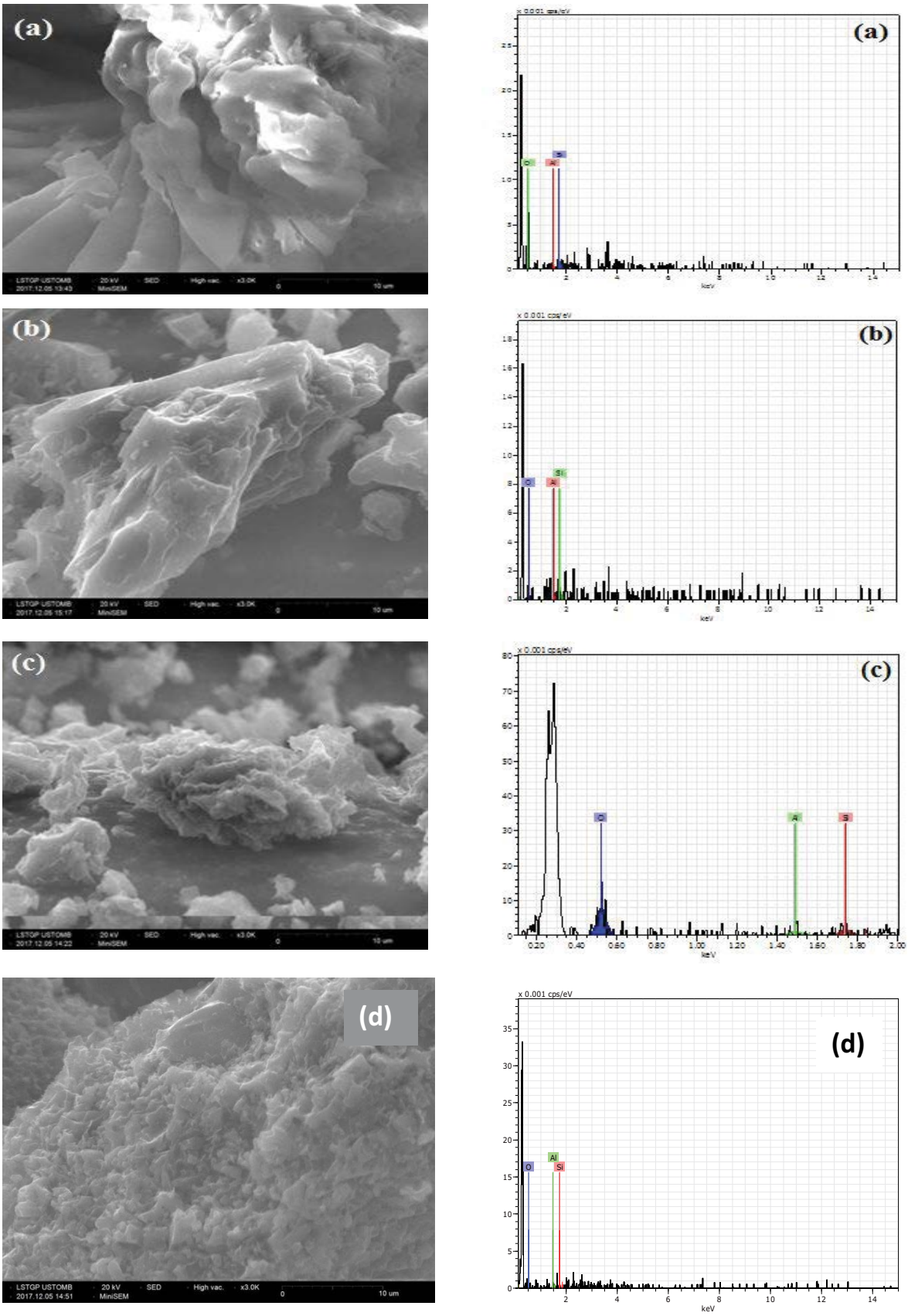

Fig. 3. EDX microanalyses and SEM images of (a) INACT, (b) AH30, (c) AC-Merck, and (d) AK30 samples.

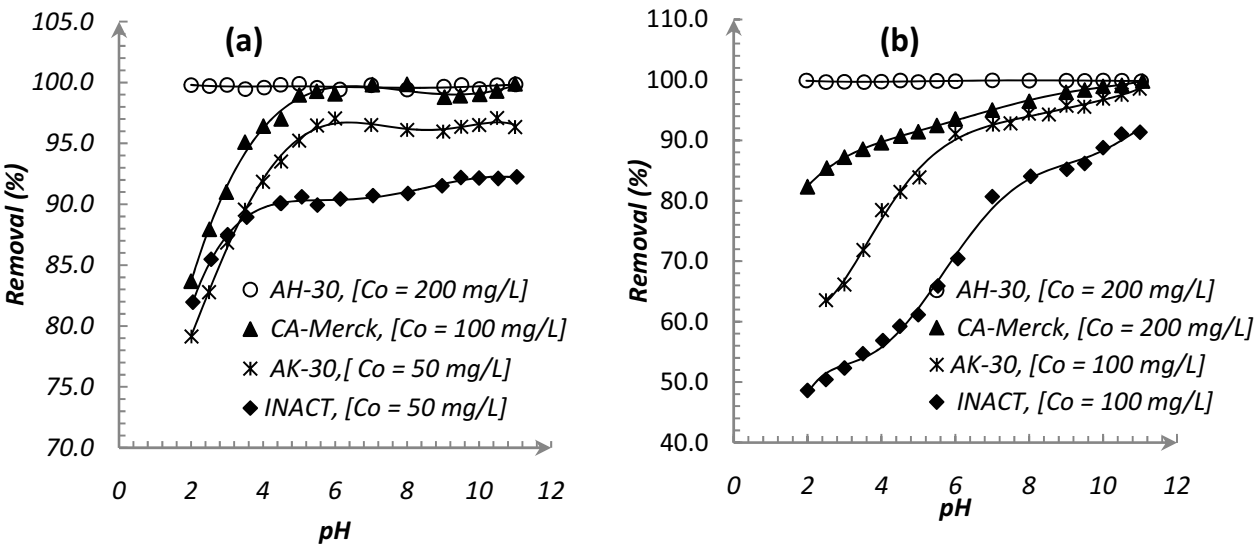

Fig. 4. pH effect on (a) Chrysoidine R and (b) Rosaniline Base and onto the different samples.

were allowed to equilibrium for time periods in excess of these values, which were assumed to be largely ample for performing all experiments.

4.3. Adsorption isotherms

In order to analyze the adsorption data and to determine the adsorption capacities of the adsorbents, an equilibrium study was performed using single-component adsorption isotherms models, namely Langmuir [37] and Freundlich [38] at previously determined operating conditions. These isotherms represented by Eqs. (3) and (4) were fitted to experimental data to describe the adsorption of Rosaniline Base and Chrysoidine R dyes at the solid–liquid interface.

4.3.1. Langmuir isotherm

Eq. (3) assumes that the adsorption process takes place at specific homogeneous sites within the adsorbent.

$$q_e = \frac{q_m b C_{\text{eq}}}{1 + b C_{\text{eq}}} \tag{3}$$

where q_e is the amount of solute adsorbed per unit weight of adsorbent (mg g^{-1}), C_{eq} is the concentration of solute remaining in solution at equilibrium (mg L^{-1}), b (mg g^{-1}) is the maximum adsorption capacity corresponding to complete monolayer coverage and K_L is a constant related to the energy via net enthalpy.

4.3.2. Freundlich isotherm

This model given by Eq. (4) is generally used to describe adsorption tests taking place on heterogeneous adsorbents and to define the exponential distribution of active sites and their energies.

$$q_e = K_F C_{\text{eq}}^{1/n} \tag{4}$$

where K_F and n are the Freundlich constants related to adsorption capacity and adsorption intensity can be obtained from the intercept and slope of logq_e vs. logC_{eq} plot.

The adsorption isotherms of both dyes onto the investigated activated carbons at working conditions determined previously such as pH, solid/liquid ratio, equilibrium time and temperature have a typical Langmuir type-I isotherm according to IUPAC classification [39]. As it can be seen from Fig. 6 that the adsorption rate increases rapidly for low concentrations in solution then attenuates to reach a plateau (saturation sites) [40] corresponding to maximum adsorption capacity values of both dyes presented in Table 4 and shown in Fig. 7.

Langmuir adsorption model is more representative for experimental data with $R^2 \geq 0.99$. It predicts an asymptotic approach to monolayer surface coverage of the adsorbents as dyes concentration approaches saturation. Preliminary adsorption tests using inactive leaves (INACT) gave encouraging results of 97.09 and 147.06 mg g^{-1} for Chrysoidine R and Rosaniline base uptakes, respectively. Enhancement of adsorption capacities by 63.48% and 142.85% for Chrysoidine R and Rosaniline base, respectively, were attained using AH30 against 17.14 and 19.29 times using AK30 adsorbent compared with their inactive state. Similar improvement by chemical treatments was reported [41]. We can conclude that AK30 and AH30 samples compare favorably with their inactivated counterparts as well as the commercial Merck activated carbon and other adsorbents reported in Table 5. The adsorptions capacities are classified as follows: [$q_{e\,(\text{INACT})} < q_{e\,(\text{AC-Merck})} < q_{e\,(\text{AK30})} < q_{e\,(\text{AH30})}$] for both dyes.

As shown in Fig. 8, Freundlich adsorption model with R^2 much low implies that this model is not representative for the experimental data. According to n values ($n > 1$) listed in Table 4, Rosaniline Base and Chrysoidine R dyes adsorption is thus correctly carried out for the four samples meaning that the adsorption processes are favorably in accordance with those reported in the literature [23,24,42].

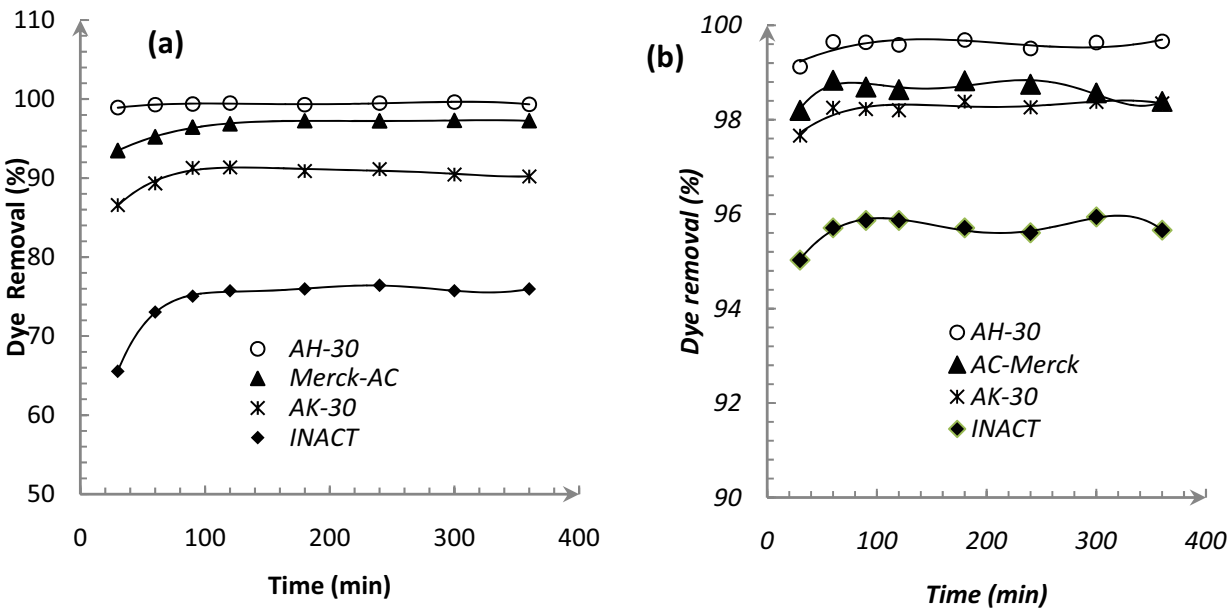

Fig. 5. Time effect (a) Chrysoidine R and (b) Rosaniline Base and onto the different samples.

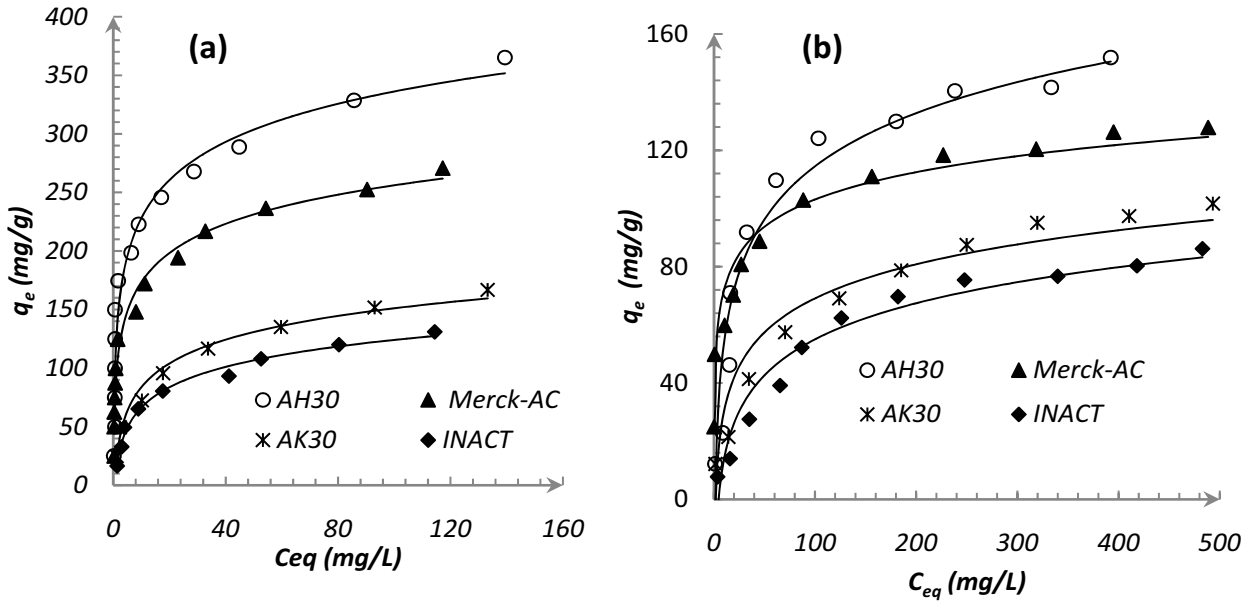

Fig. 6. Adsorption isotherms of (a) Rosaniline Base and (b) Chrysoidine R onto the different samples.

4.4. Adsorption kinetics

For kinetic study, volumes of 50 mL of dye solutions of known concentration were introduced separately in 100 mL conical flasks to which an optimized amount of the prepared adsorbents was added (m_{AH30} = 0.2 g, m_{AK30} = 0.2 g, $m_{Merck\text{-}AC}$ = 0.2 g and m_{INACT} = 0.3 g). The mixtures were stirred at 600 rpm for different times ranging from 15 to 120 min. After filtering, the final concentrations corresponding to time t were determined by spectrophotometer and uptake (mg g^{-1}) using Eq. (2).

Among the commonly used kinetic models, the pseudo-first-order kinetic model [43], the pseudo-second-order kinetic model [44] and the intra-particle diffusion model [45] were used to test the experimental data and to evaluate the kinetic mechanism for dyes adsorption onto solid adsorbents. For this purpose, an optimized amount of each adsorbent was introduced into a 25 mL-dyes solution and the adsorbed amount was monitored as a function of equilibrium contact time determined previously [46]. These models are summarized in Table 6 and were tested for our data and their validity was verified by linear equation plots

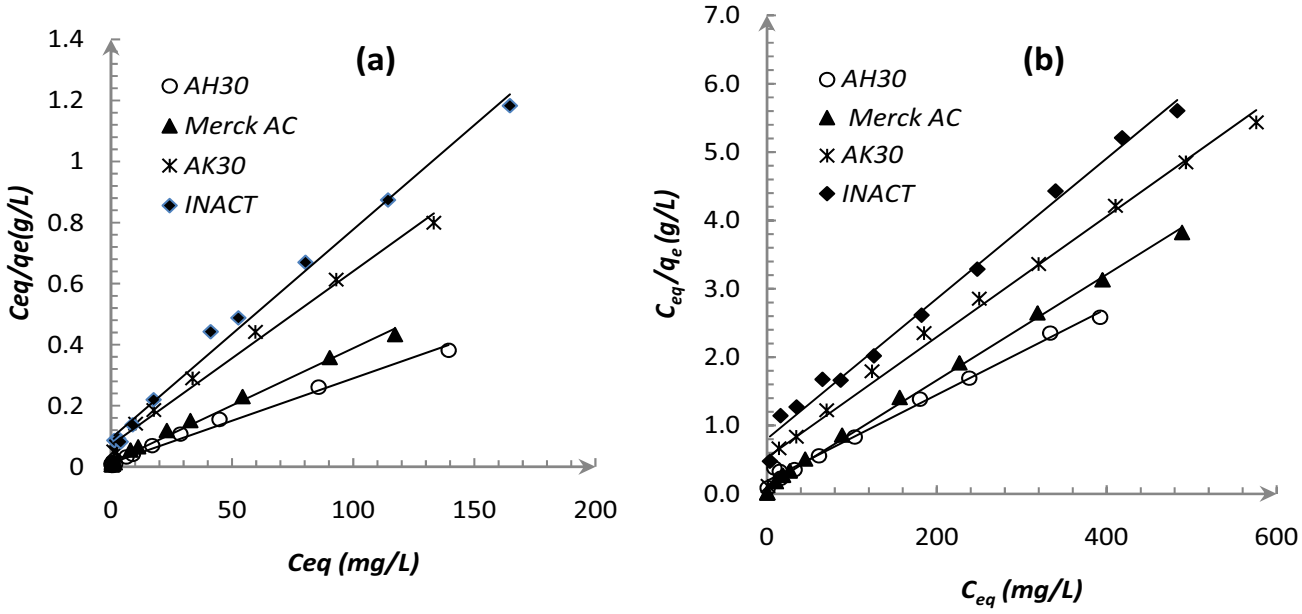

Fig. 7. Langmuir isotherm for adsorption of (a) Rosaniline Base and (b) Chrysoidine R.

Table 5
Comparison of the adsorption capacities of various adsorbents for Chrysoidine R, and Rosaniline Base uptake

Adsorbents	Pollutants	q_{max} (mg g^{-1})	Reference
Sawdust activated	Chrysoidine R	33.33	[26]
Bottom ash	Chrysoidine R	18.08	[24]
IONPs	Chrysoidine R	59.10	[23]
CI	Chrysoidine R	110.90	[23]
IONPs-CI	Chrysoidine R	126.60	[23]
Inactivated *Olea europaea* leaves	Chrysoidine R	97.09	This work
Merck-AC	Chrysoidine R	129.87	This work
H_2SO_4/*Olea europaea* leaves	Chrysoidine R	158.73	This work
Mussel shell material (CMS)	Rosaniline Base	141.65	[48]
Raw *Pistachio Nutshells* (RPNS)	Rosaniline Base	118.20	[29]
HCl-modified *mash* (HMM)	Rosaniline Base	58.48	[41]
Iodopolyurethane (Iodo-PUP)	Rosaniline Base	267.40	[49]
Inactivated *Olea europaea* leaves	Rosaniline Base	147.06	This work
Merck-AC	Rosaniline Base	270.27	This work
H_2SO_4/*Olea europaea* leaves	Rosaniline Base	357.14	This work

analysis as principal criterion, where q_e and q_t (mg g^{-1}) are the amount of dye adsorbed at equilibrium and at time t (min), respectively, k_1 (min^{-1}) is the adsorption rate constant, t (min) is the contact time. k_2 (g mg^{-1} min^{-1}) is the rate constant of second order equation. k_{int} (mg g^{-1} min$^{-1/2}$) is the intra-particle diffusion rate constant, and C (mg g^{-1}) is a constant that gives an idea about the boundary layer thickness.

In order to describe the adsorption mechanism of Chrysoidine R and Rosaniline Base, adsorption rate constants were calculated using Eqs. (5)–(7). The low values of R^2 (Table 7) and the difference between q_e (exp) and q_e (calc) indicate that the pseudo-first-order model was not well suited for describing the adsorption of both dyes used in this study. On the other hand, both higher R^2 values and the similarity of q_e (exp) and q_e (calc) indicate that pseudo-second-order model successfully describe the kinetics of both dyes adsorption by all considered adsorbents as shown in Fig. 9. Weber's intra-particle diffusion model expressed by Eq. (7) was also applied to the obtained data to elucidate the diffusion mechanism. Fig. 10 shows the linear plot of q_t vs. $t^{0.5}$ from which the intercept (C) reflecting the boundary layer effect and the intra-particle rate constant (k_{int}) values were evaluated and presented in Table 7. The larger is the value of C, the greater is the boundary

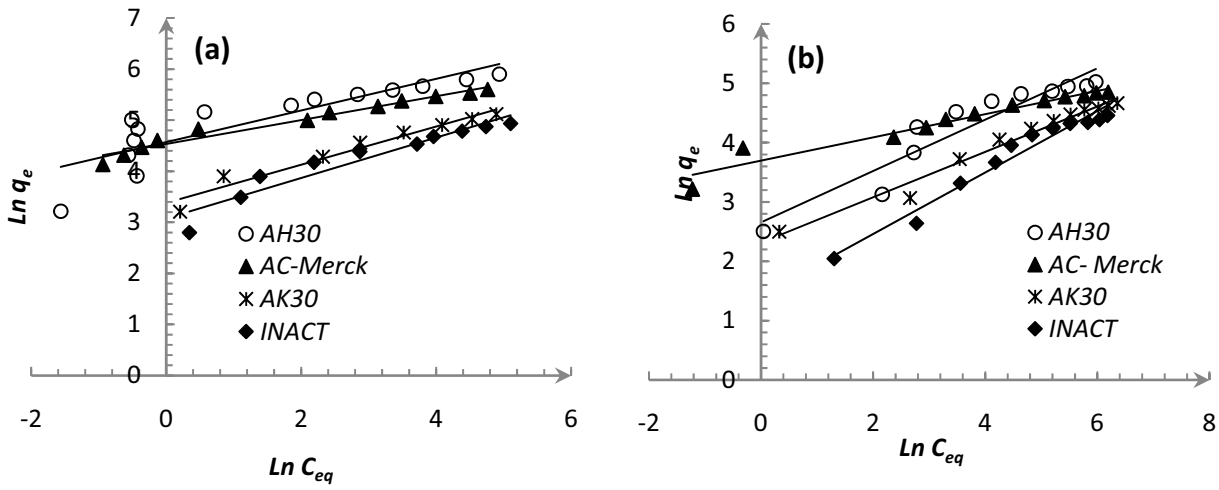

Fig. 8. Freundlich isotherm for adsorption of (a) Rosaniline B and (b) Chrysoidine R.

Table 6
Kinetic models equations used in this study

Model	Equations		Plots	Parameters
Pseudo-first-order	$\ln(q_e - q_t) = \ln q_e - k_1 \cdot t$	(5)	log $(q_e - q_t)$ vs. t	q_e: from the intercept k_1: from the slope
Pseudo-second-order	$\frac{t}{q_t} = \frac{1}{k_2 q_{e,2}^2} + \frac{1}{q_e} t$	(6)	t/q_t vs. t	q_e: from the intercept k_2: from the slope
Intra-particle diffusion	$q_t = k_{\text{int}}\, t^{0.5} + C$	(7)	q_t vs. $t^{0.5}$	C: from the intercept k_{int}: from the slope

layer effect. Straight lines obtained by q_t vs. $t^{0.5}$ plots shown in Fig. 10 indicate well that the sorption processes were also controlled by intra-particle diffusion.

4.5. Thermodynamic study

Thermodynamic functions such as changes in the standard free energy ($\Delta G°$), the enthalpy ($\Delta H°$) and entropy ($\Delta S°$) were evaluated graphically by varying the adsorption temperature in order to understand the thermodynamic behavior of both dyes adsorption onto the investigated adsorbents. These functions were calculated from the adsorption distribution coefficient (K_d) using the following equations:

$$K_d = \frac{q_e}{C_e} \tag{8}$$

$$\ln K_d = \frac{\Delta S°}{R} - \frac{\Delta H°}{T} \tag{9}$$

$$\Delta G° = -RT \ln K_d = T\Delta S° - \Delta H° \tag{10}$$

Fig. 11 shows plots of $\ln K_d$ vs. T^{-1} from which $\Delta S°$ and $\Delta H°$ are obtained from the intercept and the slope, respectively. Thermodynamic function values are summarized in Table 8.

Negative values of $\Delta G°$ indicate that nature of both dyes adsorption onto the used adsorbents at different temperature is spontaneous. In all cases, the negative values of $\Delta H°$ are an indication that adsorption processes of both dyes were taken place exothermically. This exothermicity is due to a decrease in the residual forces on adsorbents surfaces, causing then a decrease in the surface energy of the adsorbent. Their magnitude is another indication associated with physisorption in most cases, where $\Delta H° <$ kJ mol^{-1} and chemisorptions for the case of adsorption of Rosaniline B onto AK30, AH30 and Merck-AC where $\Delta H° >$ 40 kJ mol^{-1}. The latter, has higher enthalpy of adsorption because the chemical bonds are much stronger. Attractive forces are responsible for holding the adsorbate on the adsorbent surface in adsorbed state. The temperature has almost no effect on the Rosaniline B dye adsorption by INACT. While the increase in temperature promotes the retention of the same dye by the other adsorbents studied. In contrast, changes in temperature affected negatively the adsorption capacities of both dyes by AH30, AK30 and AC-Merck adsorbents. This may be due to the nature of interactions dye–adsorbents. In other words, temperature increase promotes the diffusion of molecules across the outer boundary layer and the internal pores of the adsorbent particles, probably due to the decrease of the viscosity of the solution which can have an effect on the adsorption capacity.

Table 7
Kinetic parameters for the adsorption of Chrysoidine R and Rosaniline Base onto the prepared samples

Dyes		Adsorbents			
		INACT	AH30	AK30	AC-Merck
Rosaniline Base	Initial Concentration (mg g^{-1})	100	200	200	200
	Pseudo-first-order				
	q_e (exp) (mg g^{-1})	16.285	49.760	24.707	46.160
	q_e (calc) (mg g^{-1})	4.390	9.530	5.970	6.230
	k_1 (min^{-1})	0.066	0.114	0.031	0.042
	R^2	0.842	0.959	0.873	0.943
	Pseudo-second-order				
	q_e (exp) (mg g^{-1})	16.258	49.760	24.707	46.160
	q_e (calc) (mg g^{-1})	16.920	50.505	24.938	47.170
	k_2 (g min^{-1} mg^{-1})	0.025	0.017	3.216	0.449
	R^2	0.998	0.999	0.998	0.999
	Intra-particle diffusion				
	q_e (calc) (mg g^{-1})	16.285	49.760	24.707	46.16
	k_{int} (mg g^{-1} $min^{-0.5}$)	0.784	0.909	0.739	0.849
	C (mg g^{-1})	10.922	43.62	18.85	39.997
	R^2	0.699	0.803	0.884	0.989
Chrysoidine R	Initial concentration (mg g^{-1})	50	100	50	100
	Pseudo-first-order				
	q_e (exp) (mg g^{-1})	7.140	24.915	12.378	22.318
	q_e (calc) (mg g^{-1})	7.310	8.583	8.979	14.021
	k_1 (min^{-1})	0.016	0.017	0.021	0.023
	R^2	0.897	0.960	0.988	0.953
	Pseudo-second-order				
	q_e (exp) (mg g^{-1})	7.140	24.915	12.378	22.318
	q_e (calc) (mg g^{-1})	7.163	24.876	12.407	23.753
	k_2 (g min^{-1} mg^{-1})	0.051	0.043	0.111	0.492
	R^2	0.983	1.000	0.999	0.993
	Intra-particle diffusion				
	q_e (calc) (mg g^{-1})	7.140	24.915	12.378	22.318
	k_{int} (mg g^{-1} $min^{-0.5}$)	0.336	0.056	0.140	1.237
	C (mg g^{-1})	3.122	24.268	10.852	8.665
	R^2	0.916	0.972	0.962	0.992

Some entropy ($\Delta S°$) values are negative suggesting that the adsorption process involves an associative mechanism and reflecting that no significant change occurs in the internal structures of the adsorbent during the adsorption process [47–50].

4. Conclusion

Different activation processes can be used to produce activated carbons from a variety of agricultural by-products. Among them, *Olea europaea* leaves, suitable raw and carbonaceous material were chosen in this investigation as a precursor for activated carbon preparation. Simultaneous activation was performed using impregnation of ground leaves separately into phosphoric acid or potassium hydroxide followed by pyrolysis at 500°C. Net improvement of adsorptive capacities up to 158.73 and 357.14 mg g^{-1} for Chrysoidine R and Rosaniline Base dyes has been noted due to treatments compared with 97.09 and 147.06 mg g^{-1} of the same dyes adsorbed onto inactivated leaves and the supplied commercial AC-Merck used as a reference under optimal working conditions. Langmuir adsorption model is more representative for the experimental data predicting then an asymptotic approach to monolayer surface coverage of the adsorbents at saturation. Adsorption processes of both dyes were taken place via physisorption associated with and spontaneity at different temperatures. Adsorption capacities were classified as: $q_{e\ (INACT)} < q_{e\ (AK30)} < q_{e\ (AC\text{-}Merck)} < q_{e\ (AH30)}$. Enhancement for AH30 and AK30 leaves compared with their inactivated state as expected. Chemical activation is preferred over physical activation owing to the lower temperatures and shorter time needed for activating

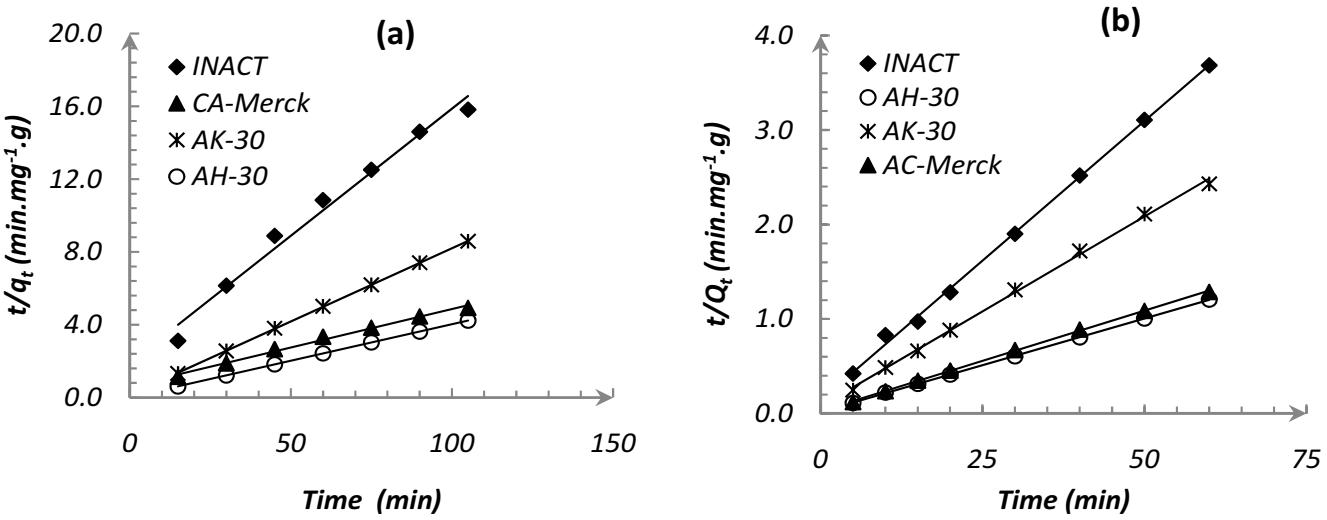

Fig. 9. Linear pseudo-second-order kinetic plots for dyes uptake on activated carbons.

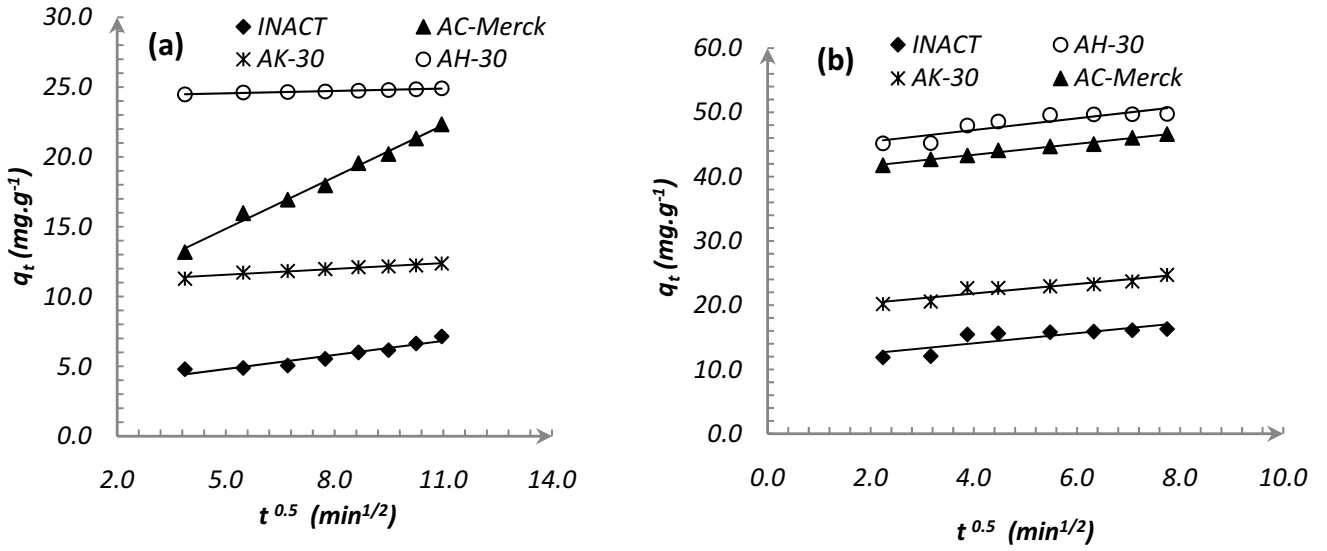

Fig. 10. Intra particle diffusion of (a) Chrysoidine R and (b) Rosaniline Base adsorption.

Table 8
Thermodynamic parameters of dyes adsorption onto the prepared adsorbents

Adsorbent	Pollutants	R^2	$-\Delta H$ (kJ mol^{-1})	ΔS (kJ mol^{-1} K^{-1})	$-\Delta G$ (kJ mol^{-1})		
					298 K	303 K	313 K
INACT	Rosaniline B	0.935	12.355	0.0274	20.412	20.395	20.787
	Chrysoidine R	0.467	16.804	–0.0111	13.175	13.949	13.155
AH30	Rosaniline B	0.986	81.495	–0.1714	30.217	29.796	27.722
	Chrysoidine R	0.964	26.370	–0.0032	25.521	25.271	25.432
AK30	Rosaniline B	0.922	46.268	–0.0822	22.009	20.976	20.667
	Chrysoidine R	0.812	16.723	0.0020	17.450	17.089	17.414
AC-Merck	Rosaniline B	0.885	37.687	–0.0486	23.489	22.619	22.652
	Chrysoidine R	0.590	3.375	0.0067	16.159	16.505	16.827

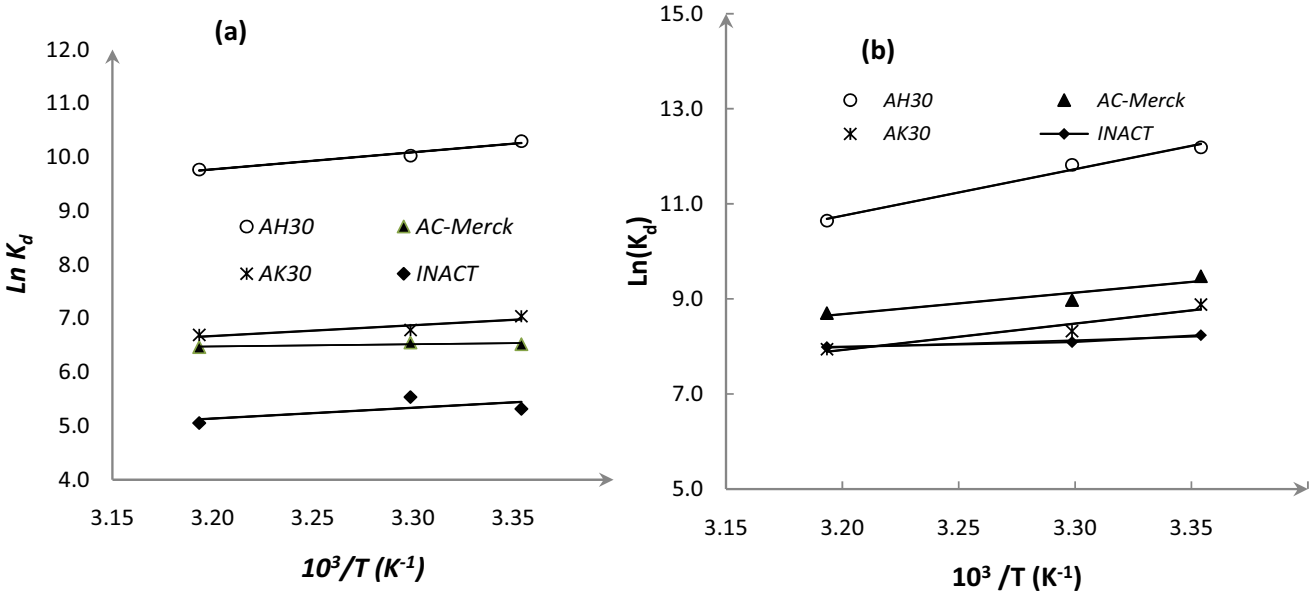

Fig. 11. Ln(K_d) as a function of temperature for thermodynamic properties determination (a) Chrysoidine (Co = 7.61 × 10^{-4} mol/L for AH30 and Co = 3.80 × 10^{-4} mol/L for AK30, Merck-AC and INACT), (b) Rosaniline Base, (Co = 5.92 × 10^{-4} mol/L for AH30 and Co = 2.96 × 10–4 mol/L for AK30, Merck-AC and INACT).

material These significant adsorption capacities showed that the activated *Olea europaea* leaves can be used as an alternative to the commercial adsorbents in removing dyestuff from textile wastewater industries.

Acknowledgment

The authors would like to thank the financial support from National PRFU project (Mostaganem University) Code: B00L01UN270120180003 01/01/2018 of the Ministry of Higher Education, Algeria.

References

[1] K.-M. Wollin, H.P.A. Illing, Limit Value Setting in Different Areas of Regulatory Toxicology, F.X. Reichl, M. Schwenk, Eds., Regulatory Toxicology, Springer, Berlin, Heidelberg, 2014, https://doi.org/10.1007/978-3-642-35374-1_81.
[2] D. Brown, Effects of colorants in the aquatic environment, Ecotox. Environ. Saf., 13 (1987) 139–147.
[3] T. Robinson, G. McMullan, R. Marchant, P. Nigam, Remediation of dyes in textile effluent: a critical review on current treatment technologies with a proposed alternative, Bioresour. Technol., 77 (2001) 247–255.
[4] S. Aoudj, A. Khelifa, N. Drouiche, M. Hecini, H. Hamitouche, Electro-coagulation process applied to wastewater containing dyes from textile industry, Chem. Eng. Process., 49 (2010) 1176–1182.
[5] T. Shu-Hui, M.A.A. Zaini, Dyes – Classification and Effective Removal Techniques, J.C. Taylor, Ed., Advances in Chemistry Research, Nova Science Publishers, Inc., New York., Vol. 30, 2016, pp. 19–34.
[6] I. Abdelfattah, F. Nasr, A. Shana, Cost-effective physicochemical treatment of carpet industrial wastewater for reuse, Egypt. J. Chem., 62 (2019) 609–620.
[7] N.K. Daud, U.G. Akpan, B.H. Hameed, Decolorization of sunzol black DN conc. in aqueous solution by Fenton oxidation process, effect of system parameters and kinetic study, Desal. Water Treat., 37 (2012) 1–7.
[8] Y. Shiva Shankar, K. Ankur, P. Bhushan, D. Mohan, Utilization of Water Treatment Plant (WTP) Sludge for Pretreatment of Dye Wastewater Using Coagulation/Flocculation, A. Kalamdhad, J. Singh, K. Dhamodharan, Eds., Advances in Waste Management, Springer, Singapore, 2019, pp. 107–121, https://doi.org/10.1007/978-981-13-0215-2_8.
[9] M.F. Abid, M.A. Zablouk, A.M. Abid-Alameer, Experimental study of dye removal fromindustrial wastewater by membrane technologiesof reverse osmosis and nanofiltration, Iran. J. Environ. Health, 9 (2012) 17.
[10] M.M. Hassan, C.M. Carr, A critical review on recent advancements of the removal of reactive dyes from dye house effluent by ion-exchange adsorbents, Chemosphere, 209 (2018) 201–219.
[11] A. Dabrowski, Adsorption-from theory to practice, Adv. Colloid Interface, 9 (2001) 135–224.
[12] R.C. Bansal, G. Meenakshi, Activated Carbon Adsorption, Taylor & Francis Group, LLC, 2005.
[13] A. Mudhoo, D. Beekaroo, Adsorption of Reactive Red 158 Dye by Chemically Treated *Cocos nucifera* L. Shell Powder, SpringerBriefs in Molecular Science, 2011, pp. 1–65.
[14] S. Ming-Twang, L. Lin-Zhi, M.A.A. Zaini, Q. Zhi-Yong, A.Y. Pei-Yee, Activated Carbon for Dyes Adsorption in Aqueous Solution, J.A. Daniels, Ed., Advances in Environmental Research, Vol. 36, Nova Science Publishers, Inc., New York., 2015, pp. 217–234.
[15] R.S. Juang, F.C. Wu, R.L. Tseng, The ability of activated clay for the adsorption of dyes from aqueous solutions, Environ. Technol., 18 (1997) 525–531.
[16] J.P. Castro, J.R.C. Nobre, A. Napoli, M.L. Bianchi, J.C. Moulin, B.S. Chiou, G.H. Tonoli, Massaranduba sawdust: a potential source of charcoal and activated carbon, Polymers., 11 (2019) 1276.
[17] B.N. Thomas, S.C. George, Production of activated carbon from natural sources, Trends Green Chem., 1 (2015) 1–7.
[18] K. Larbi, N. Benderdouche, L. Reinert, J.M. Leveque, S. Delpeux, M. Benadjemia, B. Bestani, L. Duclaux, Tailored activated carbons prepared by phosphoric activation of apricot, date and loquat stones and their mixtures; relation between the pore

size and the composition in biopolymer, Desal. Water Treat., 120 (2018) 217–227.
[19] J. Junaid Saleem, U. Bin Shahid, M. Hijab, H. Mackey, G. McKay, Production and applications of activated carbons as adsorbents from olive stones, Biomass Convers. Biorefin., 9 (2019) 775–802.
[20] N. Benderdouche, B. Bestani, B. Benstaali, Z. Derriche, Enhancement of the adsorptive properties of a desert *Salsola Vermiculata* species, Adsorpt. Sci. Technol., 21 (2003) 739–750.
[21] N. Douara, B. Bestani, N. Benderdouche, L. Duclaux, Sawdust-based activated carbon ability in the removal of phenol-based organics from, Desal. Water Treat., 57 (2015) 5529–5545.
[22] A. Ouldmoumna, L. Reinert, N. Benderdouche, B. Bestani, L. Duclaux, Characterization and application of three novel biosorbents "*Eucalyptus globulus*, *Cynara cardunculus* and *Prunus cerasefera*" to dye removal, Desal. Water Treat., 51 (2013) 3527–3538.
[23] D.L. Han, P.A. Cao, M. Popa, H. Nguyen Xuan, Hybrid composite based on magnetite/chitosan for 2,4-d and chrysoidine removal, Vietnam. J. Sci. Technol., 56 (2018) 184.
[24] M. Matheswaran, T. Karunanithi, Adsorption of Chrysoidine R by using fly ash in batch process, J. Hazard. Mater., 145 (2007) 154–161.
[25] M.K. Purkait, D.S. Gusain, S. Das Gupta, S. De, Adsorption Behavior of Chrysoidine dye on activated charcoal and its regeneration characteristics by using different surfactants, Sep. Sci. Technol., 39 (2005) 2419–2440.
[26] M.W. Ashraf, N. Abulibdeh, A. Salam, Adsorption studies of textile dye (Chrysoidine) from aqueous solutions using activated sawdust, Int. J. Chem. Eng., 2019 (2019) 1–8.
[27] V.M. Nurchi, M. Crespo-Alonso, R. Biesuz, G. Alberti, M.I. Pilo, N. Spano, G. Sanna, Sorption of chrysoidine by row cork and cork entrappedin calcium alginate, Arab. J. Chem., 7 (2014) 133–138.
[28] S.K. Goyal, Use of rosaniline hydrochloride dye for atmospheric SO_2 determination and method sensitivity analysis, J. Environ. Monit., 3 (2001) 666–670.
[29] M. El-Azazy, A.S. El-Shafie, A. Ashraf, A.A. Issa, Eco-structured biosorptive removal of Basic Fuchsin using pistachio nutshells: a definitive screening design—based approach, Appl. Sci., 9 (2019) 4855.
[30] B. Bestani, N. Benderdouche, B. Benstaali, A. Addou, Adsorption of Methylene Blue and iodine from aqueous solutions by a desert *Salsola vermiculata* species, Bioresources, 99 (2008) 8441–8444.
[31] ASTM, Standard Test Method for Determination of Iodine Number of Activated Carbon, ASTM Annual Book, Vol. 4, 1999, D4607–94, Section 15.
[32] A. Belayachi, B. Bestani, A. Bendraoua, N. Benderdouche, L. Duclaux, The influence of surface functionalization of activated carbon on dyes and metal ion removal from aqueous media, Desal. Water Treat., 57 (2015) 17557–17569.
[33] C. Kaewprasit, E. Hequet, N. Abidi, J.P. Gourlo, Application of Methylene Blue adsorption to cotton fiber specific surface area measurement: Part I. methodology, J. Cotton. Sci., 2 (1998) 164–173.
[34] H.P. Boehm, Surface oxides on carbon and their analysis: a critical assessment, Carbon, 40 (2002) 145–149.
[35] L.H. Noszko, A. Bota, A. Simay, L.G. Nagy, Preparation of activated carbon from the by-products of agricultural industry, Periodica Polytechnica Chem. Eng., 28 (1984) 293–297.
[36] A. Cleiton, C. Nunes e Mario, Guerreiro, Estimation of surface area and pore volume of activated carbons by methylene blue and iodine numbers, Quim. Nova, 34 (2011) 472–476.
[37] I. Langmuir, The constitution and fundamental properties of solids and liquids, J. Am. Chem. Soc., 38 (1916) 2221–2295.
[38] H.M.F. Freundlich, Uber die adsorption in losungen, Zeitschrift Physikalische Chemie., 57 (1906) 385–470.
[39] K.S.W. Sing, D.H. Everett, R.A.W. Haul, L. Moscou, R.A. Pieroti, J. Rouquerol, T. Siemieniewska, Reporting physisorption data for gas/solid systems with special reference to the determination of surface area and porosity, Pure Appl. Chem., 57 (1985) 603–619.
[40] L.M. Sun, F. Meunier, Adsorption. Theoretical aspects. Engineering techniques - unit operations - chemical reaction engineering, Proc. Eng. Treaty J., 2730 (2003).
[41] SUN, Lian-Ming et MEUNIER, Francis, Adsorption, Aspects théoriques, Techniques de l'ingénieur, Génie des procédés, 2003, vol. 2, N° J2730, 1–16.
[42] A. Mittal, J. Mittal, A. Malviya, V.K. Gupta, Removal and recovery of Chrysoidine Y from aqueous solutions by waste materials, J. Colloid Interface Sci., 34 (2010) 497–507.
[43] S. Lagergren, Zur theorie der sogenannten adsorption geloester stoffe. K. Sven. Vetenskapsakad. Handl., 24 (1898) 1–39.
[44] Y.S. Ho, G. McKay, The kinetics of sorption of divalent metal ions onto sphagnum moss peat, Water Res., 34 (2000) 735–742.
[45] W.J. Weber Jr., J.C. Morris, Kinetics of adsorption on carbon from solution, J. Sanitary Eng. Div. Proceed. Am. Soc. Civil Eng., 89 (1963) 31–59.
[46] S. Attouti, B. Bestani, N. Benderdouche, L. Duclaux, Application of *Ulva lactuca* and *Systoceira stricta* algae-based activated carbons to hazardous cationic dyes removal from industrial effluents, Water Res., 47 (2013) 3375–3388.
[47] F. Nemchi, B. Bestani, N. Benderdouche, M. Belhakem, L. Duclaux, Enhancement of Ni^{2+} removal capacity of activated carbons obtained from Mediterranean *Ulva lactuca* and *Systoceira stricta* algal species, J. Environ. Chem. Eng., 5 (2017) 2337–2345.
[48] Z. Derikvand, S. Akbari, G. Kouchakzadeh, A. Azadbakht, A. Nemati, High performance removal of Azo and cationic dyes pollutants with Mn-aluminophosphate particles: kinetics, thermodynamics, and adsorption equilibrium studies, Russ. J. Phys. Chem. A, 93 (2019) 2604–2612.
[49] M. El Haddad, Removal of Basic Fuchsin dye from water using mussel shell biomass waste as an adsorbent: equilibrium, kinetics, and thermodynamics, J. Taibah Univ. Sci., 10 (2016) 664–674.
[50] E.A. Moawed, M.F. El-Shahat, Equilibrium, kinetic and thermodynamic studies of the removal of triphenyl methane dyes from wastewater using iodopolyurethane powder, J. Taibah Univ. Sci., 10 (2016) 46–55.